

Design of Joint Position and Constellation Mapping Assisted DCSK Scheme Subject to Laplacian Impulsive Noise

Xiangming Cai, Weikai Xu, *Member, IEEE*, Lin Wang, *Senior Member, IEEE*, Guanrong Chen, *Life Fellow, IEEE*

Abstract—In this letter, a joint position and constellation mapping (JPCM) assisted differential chaos shift keying (JPCM-DCSK) scheme is proposed to address the problem of unreliable data transmission in the power line communication (PLC) channel subjected to Laplacian impulsive noise. The constellation states and time slot position patterns are integrated cooperatively, which enables JPCM-DCSK to transmit more information bits. An effective JPCM detection algorithm is proposed to recover the information bits. Moreover, the bit error rate (BER) expression of JPCM-DCSK is derived over a multipath PLC channel, which is verified by computer simulations. Comparisons of BER performances demonstrate that JPCM-DCSK outperforms its competitors by 2 dB to 6 dB gains.

Index Terms—Power line communication (PLC), differential chaos shift keying (DCSK), Laplacian impulsive noise.

I. INTRODUCTION

Power line communication (PLC) uses medium and low voltage electrical networks to provide telecommunication services [1]. The orthogonal frequency division multiplexing (OFDM) is used in PLC to reduce the effects of multipath fading and impulsive noise [2]. Then, the bit error rate (BER) of a binary phase shift keying (BPSK) scheme over a PLC channel with impulsive noise was studied in [3]. However, these schemes require channel state information (CSI) to combat multipath fading, which incurs infrastructure overheads.

The differential chaos shift keying (DCSK), implementable with off-the-shelf electronic circuits without requiring CSI, was proposed in [4] and further modified to adapt to PLC scenarios in [5]. Then, a replica piecewise M -ary DCSK (RP-MDCSK) was presented in [6] to reduce the adverse effect of asynchronous impulsive noise. Note that the suppression of impulsive noise in RP-MDCSK is at the cost of low energy efficiency. To improve the data rate, great efforts were devoted to combining index modulation with DCSK [7]–[9].

Generally, impulsive noise occurs in form of a burst and its intensity is quite high [10], [11]. The detrimental effects of different types of impulsive noise on the BER performance of PLC were discussed in [12]. According to [13], [14], the probability density function (PDF) of impulsive noise approaches zero more slowly compared to that of Gaussian

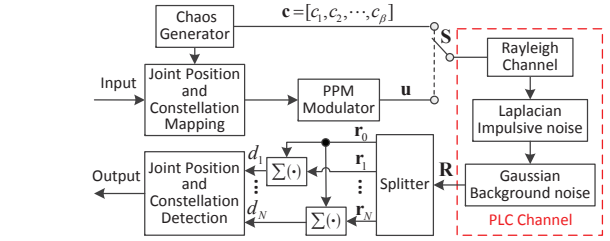


Fig. 1. Block diagram of the JPCM-DCSK system.

distribution, therefore impulsive noise can be better modeled by using the Laplace distribution.

In order to address the problem of unreliable data transmission in the PLC channel subjected to Laplacian impulsive noise, a joint position and constellation mapping assisted DCSK (JPCM-DCSK) system is proposed in this letter. JPCM-DCSK is based on single-carrier modulation, and it operates in the frequency range from 5 kHz to 500 kHz, which is typical for narrowband PLC. Different from the works in [2], [13], [14], JPCM-DCSK can reduce the adverse effect of multipath fading without requiring CSI, thereby reducing the system complexity. Different from RP-MDCSK, JPCM-DCSK has superior robustness in the PLC channel without penalizing the energy efficiency. In JPCM-DCSK, the positions of information-bearing time slots and the constellation of BPSK modulated symbol are jointly mapped to a stream of transmitted bits, so that additional information bits are transmitted by JPCM-DCSK. An effective joint position and constellation detection algorithm is developed to determine the time slot position patterns (TSPPs) and the information bits are retrieved by these TSPPs. The BER expression of JPCM-DCSK is derived over the multipath PLC channel subjected to Laplacian impulsive noise. The BER performance comparisons demonstrate that JPCM-DCSK can offer 2 to 6 dB gains and its error floor is lower compared to RP-MDCSK and DPI-DCSK.

In Section II, the system model is introduced. Performance analysis is given in Section III, followed by simulation results in Section IV. Finally, Section V concludes the paper.

II. SYSTEM MODEL

In this section, the system model of JPCM-DCSK is presented. The principle of joint position and constellation mapping and the corresponding detection algorithm are presented.

Fig. 1 shows the block diagram of JPCM-DCSK. The time slot positions and constellation states are jointly mapped to the transmitted bits in a one-to-one manner. Suppose that p out of N time slots are possibly selected to carry the information-bearing signals and the remaining $N - p$ time slots

This work was supported in part by the National Natural Science Foundation of China under Grant 61671395 and Grant 61871337.

Xiangming Cai, Weikai Xu and Lin Wang are with the Department of Information and Communication Engineering, Xiamen University, Xiamen, P. R. China. (e-mail: samson0102@qq.com, xweikai@xmu.edu.cn, wanglin@xmu.edu.cn).

G. Chen is with the Department of Electrical Engineering, City University of Hong Kong, Hong Kong, P. R. China. (e-mail: eegchen@cityu.edu.hk).

keep unused. Note that p is a varying value in range $[1, P]$ ($P < N$). Consequently, there are $\kappa = \sum_{p=1}^P C(N, p)$ TSPPs in total, where $C(\cdot, \cdot)$ stands for the binomial coefficient. When the transmission of BPSK modulated symbols is considered, the total number of possible transmitted information-bearing signals is $K = \sum_{p=1}^P 2^p C(N, p)$. The number of transmitted bits can be calculated as $\partial = \lfloor \log_2 K \rfloor$, where $\lfloor \cdot \rfloor$ is the floor function. Thus, the total number of TSPPs used for information transmission is given by $Z = 2^\partial$. For a better illustration, Table I shows the relationship of the joint position and constellation mapping to the information-bearing signals in JPCM-DCSK when $N = 4$ and $P = 2$. The total number of transmitted bits is computed as $\partial = \lfloor \log_2 \sum_{p=1}^2 2^p C(4, p) \rfloor = 5$.

At the transmitter, the second-order Chebyshev polynomial function (CPF) is used in the chaos generator to produce chaotic signals. Before being processed by the pulse position modulation (PPM) modulator, the chaotic signal and input bits are loaded into the block of joint position and constellation mapping (JPCM) to get TSPPs. The transmitted signal of the JPCM-DCSK system is expressed as

$$\mathbf{S} = \begin{bmatrix} \mathbf{c} & \mathbf{u} \\ \text{reference signal} & \text{information-bearing signal} \end{bmatrix}, \quad (1)$$

where $\mathbf{c} = [c_1, c_2, \dots, c_\beta]$ denotes a length- β chaotic signal, and $\mathbf{u} = [\mathbf{0}_{1 \times \beta}, a_1 \mathbf{c}, \dots, \mathbf{0}_{1 \times \beta}, a_p \mathbf{c}]_{1 \times N\beta}$ is the information-bearing signals determined by JPCM, where $\mathbf{0}_{1 \times \beta}$ is a length- β zero vector, and $a_p = \pm 1$ is the BPSK modulated symbol.

Generally, impulsive noise originates from the unpredictable switching transients in electrical appliances plugged into the power line [15]. This kind of noise induces dramatically deleterious effect on the performance of a PLC system [2]. It has been shown that the impulsive noise can be modeled to follow a Laplacian distribution with heavy tail behavior [13], [14]. Different from other impulsive noise models, such as Middleton class A and symmetric α -stable ($S\alpha S$) distribution [12], the Laplacian distribution is a simpler model to show the high-peak and short-tail behavior of impulsive noise [16]. The received signal of the JPCM-DCSK system is formulated as

$$\mathbf{R} = \sum_{l=1}^L \alpha_l \mathbf{S}_{\tau_l} + \mathbf{n}_B + \phi \mathbf{n}_I, \quad (2)$$

where L gives the number of paths for multipath propagation, α_l and τ_l are the channel coefficient and delay of the l -th path, respectively, α_l follows a Rayleigh distribution, \mathbf{n}_B is Gaussian background noise with zero mean and power spectral density of $N_0/2$, \mathbf{n}_I is Laplacian impulsive noise, having zero mean and $2v^2$ variance, ϕ is a Poisson process describing the arrival of the impulsive noise, and the term $\phi \mathbf{n}_I$ can be physically interpreted as each transmitted sequence being hit independently by impulsive noise with a Poisson distribution.

At the receiver, the received signal \mathbf{R} is firstly split to one reference signal \mathbf{r}_0 and N information-bearing signals $\{\mathbf{r}_1, \mathbf{r}_2, \dots, \mathbf{r}_N\}$. Then, the resultant reference signal is correlated with the i -th information-bearing signal to obtain $d_i = \mathbf{r}_0(\mathbf{r}_i)^T$, $i = 1, 2, \dots, N$, where $(\cdot)^T$ denotes the transposition. Next, a joint position and constellation detection algorithm is proposed to retrieve the TSPP used at the

TABLE I
RELATIONSHIP OF JPCM TO INFORMATION-BEARING SIGNALS IN JPCM-DCSK WHEN $N = 4$ AND $P = 2$

Z	Bits	TSPPs	Information-Bearing Signals
1	00000	[1, 0, 0, 0]	[+c, 0, 0, 0]
2	00001	[1, 0, 0, 0]	[-c, 0, 0, 0]
\vdots	\vdots	\vdots	\vdots
7	00110	[0, 0, 0, 1]	[0, 0, 0, +c]
8	00111	[0, 0, 0, 1]	[0, 0, 0, -c]
9	01000	[1, 1, 0, 0]	[+c, +c, 0, 0]
10	01001	[1, 1, 0, 0]	[+c, -c, 0, 0]
\vdots	\vdots	\vdots	\vdots
31	11110	[0, 0, 1, 1]	[0, 0, -c, -c]
32	11111	[0, 0, 1, 1]	[0, 0, -c, +c]

Algorithm 1 Joint Position and Constellation Detection

Input: $\mathbf{d} = [|d_1|, |d_2|, \dots, |d_N|]$;
1: $\psi = \text{count} \{ \mathbf{d} > \frac{1}{2} d_{max} \}$, where $d_{max} = \max\{\mathbf{d}\}$;
2: $[i_1, i_2, \dots, i_\psi] = \text{find} \{ \mathbf{d}, \psi \}$;
3: $\mathbf{G} = [g_1, g_2, \dots, g_N]$, where $g_j = \begin{cases} 1, & j \in \{i_1, i_2, \dots, i_\psi\} \\ 0, & \text{otherwise} \end{cases}$;
Output: TSPP \mathbf{G} .

transmitter. The MATLAB pseudo-code of the algorithm is shown in Algorithm 1. Algorithm 1 is initialized by a length- N vector \mathbf{d} . Line 1 gives the number of elements in vector \mathbf{d} that are greater than a half of d_{max} , where $d_{max} = \max\{\mathbf{d}\}$ is the maximum element in vector \mathbf{d} . Line 2 finds ψ maximums from the elements of \mathbf{d} and records their indices as $[i_1, i_2, \dots, i_\psi]$. Subsequently, the TSPP \mathbf{G} is obtained, where each of its entries is either 0 or 1 determined by the resultant indices $[i_1, i_2, \dots, i_\psi]$ in Line 3. Finally, the transmitted bits are estimated by converting vector \mathbf{G} to binary bits according to the reverse mapping relation corresponding to Table I.

III. PERFORMANCE ANALYSIS

In this section, the final BER expression of JPCM-DCSK over an L -path Rayleigh fading PLC channel is derived. In addition, the data rate and energy efficiency of JPCM-DCSK are analyzed.

A. BER Performance Analysis

The Poisson distribution gives a good description for the occurrence of impulsive noise. Given the Poisson process with a rate of λ units per second, the probability distribution for the event of k arrivals in t seconds is obtained as $P_k(t) = \frac{(\lambda t)^k}{k!} e^{-\lambda t}$, $k = 1, 2, \dots$. According to [2], the occurrence probability of impulsive noise in the duration time of the transmitted symbol is given by $P_i = \lambda T_p$, where T_p denotes the duration time of impulsive noise.

When impulsive noise occurs with probability P_i , the bit error probability of JPCM-DCSK is calculated as

$$P_T = P_i P_I + (1 - P_i) P_B = \lambda T_p P_I + (1 - \lambda T_p) P_B, \quad (3)$$

where P_I is the BER in the scenarios with both impulsive noise and background noise while P_B is the BER only in

TABLE II
MEANS AND VARIANCES OF d_i AND \hat{d}_j

DVs	Means	Variances
d_i	$\mu = \frac{E_s}{1+p}$	$\sigma_1^2 = \frac{E_s N_0}{1+p} (1 + \aleph) + \beta (1 + \aleph)^2 \frac{N_0^2}{4}$
\hat{d}_j	0	$\sigma_2^2 = \frac{E_s N_0}{2(1+p)} (1 + \aleph) + \beta (1 + \aleph)^2 \frac{N_0^2}{4}$

the presence of background noise. According to (3), to obtain the error probability P_T , two error probabilities P_I and P_B are necessary. Therefore, P_I and P_B will be derived in the following subsections 1) and 2), respectively.

1) BER subject to both impulsive noise and background noise P_I : Since the number of time slots used to transmit the information-bearing signals is changed from 1 to P , the energy of the transmitted signal is varied as well. Suppose that there are p time slots used to transmit information-bearing signals so that the symbol energy of JPCM-DCSK is computed as $E_s = (1+p) \sum_{l=1}^L \alpha_l^2 \mathbf{c}(\mathbf{c})^T$. The JPCM-DCSK receiver has two different tasks to recover the TPSS according to Algorithm 1. The predominant task is to determine ψ . Let the probability of erroneously detecting ψ be denoted by P_ψ . Based on the first task, the receiver needs to locate ψ possible positions of time slots that transmit information data. Let the error probability of this event be denoted by P_d . The derivations of P_ψ and P_d are as follows.

When the receiver detects the time slot carrying information data, the decision variable (DV) is given by $d_i = (\sum_{l=1}^L \alpha_l \mathbf{c} + \mathbf{n}_r)(\sum_{l=1}^L \alpha_l \mathbf{c} + \mathbf{n}_i)^T$, where $\mathbf{n}_r = \mathbf{n}_B^r + \phi \mathbf{n}_I^r$ and $\mathbf{n}_i = \mathbf{n}_B^i + \phi \mathbf{n}_I^i$ denote the noises imposed on the reference and the i -th information-bearing signals, respectively. They have the same zero means and $N_0/2 + N_I$ variances, where $N_I = 2v^2$ denotes the variance of the Laplacian impulsive noise. Let $\aleph = N_I/(N_0/2)$ be the ratio of impulsive noise power to Gaussian background noise power. The mean and variance of d_i are given in Table II. Therefore, the PDF and cumulative distribution function (CDF) of $|d_i|$ are expressed as $f_{|d_i|}(x) = \frac{1}{\sqrt{2\pi\sigma_1^2}} \{ \exp[-\frac{(x-\mu)^2}{2\sigma_1^2}] + \exp[-\frac{(x+\mu)^2}{2\sigma_1^2}] \} = f(x|\mu, \sigma_1^2)$ and $F_{|d_i|}(x) = \frac{1}{2} [\text{erf}(\frac{x-\mu}{\sqrt{2\sigma_1^2}}) + \text{erf}(\frac{x+\mu}{\sqrt{2\sigma_1^2}})] = F(x|\mu, \sigma_1^2)$, where $\text{erf}(x) = \frac{2}{\sqrt{\pi}} \int_0^x e^{-t^2} dt$, $x \geq 0$ is the error function. The CDF of d_{max} is $F_{d_{max}}(x) = F(x|\frac{1}{2}\mu, \frac{1}{4}\sigma_1^2)$.

According to [7], [8], the probability of erroneously detecting ψ can be formulated as

$$P_\psi = 1 - \Pr \left\{ |d_1| > \varpi, \dots, |d_p| > \varpi \mid p, \varpi = \frac{1}{2} d_{max} \right\} \\ = \int_0^\infty \left\{ 1 - \left[F \left(x \mid \frac{1}{2}\mu, \frac{1}{4}\sigma_1^2 \right) \right] \right\} \\ \times p [1 - F(x|\mu, \sigma_1^2)]^{p-1} f(x|\mu, \sigma_1^2) dx. \quad (4)$$

The DV corresponding to an unused time slot is given by $\hat{d}_j = (\sum_{l=1}^L \alpha_l \mathbf{c} + \mathbf{n}_r)(\mathbf{n}_j)^T$ for which the mean and variance are also shown in Table II. The error probability of time slot position detection is [7]

$$P_d = \int_0^\infty \left\{ 1 - [F(x|0, \sigma_2^2)]^{N-p} \right\} \\ \times p [1 - F(x|\mu, \sigma_1^2)]^{p-1} f(x|\mu, \sigma_1^2) dx. \quad (5)$$

The bit error probability of JPCM-DCSK, when p time slots are used to carry information data subject to impulsive noise

and background noise, is given by

$$P_{I,p} \approx \frac{1}{2} P_\psi + (1 - P_\psi) \frac{2^{\lfloor \log_2 C(N,p) \rfloor - 1}}{2^{\lfloor \log_2 C(N,p) \rfloor} - 1} P_d. \quad (6)$$

When all the values of p (ranging from 1 to P) are considered, the BER of JPCM-DCSK in the scenarios with impulsive noise and background noise can be computed as

$$P_I = \sum_{p=1}^P \frac{2^p C(N,p)}{K} P_{I,p}. \quad (7)$$

2) BER in the scenarios with background noise P_B : When only the Gaussian background noise is considered, the noise terms \mathbf{n}_r and \mathbf{n}_i become $\tilde{\mathbf{n}}_r = \mathbf{n}_B^r$ and $\tilde{\mathbf{n}}_i = \mathbf{n}_B^i$, respectively. In this case, the means and variances of d_i and \hat{d}_j are calculated as $\tilde{\mu}_1 = \frac{E_s}{1+p}$, $\tilde{\mu}_2 = 0$, $\tilde{\sigma}_1^2 = \frac{E_s N_0}{1+p} + \beta \frac{N_0^2}{4}$ and $\tilde{\sigma}_2^2 = \frac{E_s N_0}{2(1+p)} + \beta \frac{N_0^2}{4}$, respectively. Substituting the above results into (4)–(7), the BER of JPCM-DCSK subject to only Gaussian background noise is approximated as

$$P_B \approx \sum_{p=1}^P \frac{2^p C(N,p)}{K} \left[\frac{1}{2} P_\psi + (1 - P_\psi) \frac{2^{\lfloor \log_2 C(N,p) \rfloor - 1}}{2^{\lfloor \log_2 C(N,p) \rfloor} - 1} P_d \right]. \quad (8)$$

After P_I and P_B are obtained according to (7) and (8), respectively, the average BER of JPCM-DCSK over an L -path Rayleigh-faded PLC channel can be expressed as [18]

$$P_T^{multi} = \int_0^\infty P_T \sum_{l=1}^L \left[\frac{1}{\bar{\gamma}_l} \left(\prod_{j=1, j \neq l}^L \frac{\bar{\gamma}_l}{\bar{\gamma}_l - \bar{\gamma}_j} \right) e^{-\frac{\gamma_s}{\bar{\gamma}_l}} \right] d\gamma_s, \quad (9)$$

where $\gamma_s = \frac{E_s}{N_0}$ is the symbol signal-to-noise ratio (SNR), and $\bar{\gamma}_l$ is the average of instantaneous symbol SNR of the l -th channel, P_T is a conditional BER of JPCM-DCSK (conditioned on the Rayleigh fading) and P_T^{multi} denotes the average BER of JPCM-DCSK over a PLC channel in the presence of Rayleigh fading. When the conditional BER, P_T , given in (3) is averaged over the Rayleigh fading channel statistics, the final BER of JPCM-DCSK, i.e., P_T^{multi} , can be obtained.

B. Upper Bound BER

The upper bound BER of JPCM-DCSK in high SNR ranges will be derived in this subsection.

In high SNR ranges, P_ψ in (4) is approximated as $P_\psi \approx \int_0^\infty \{ 1 - [F(x|\frac{1}{2}\mu, \frac{1}{4}\sigma_1^2)] \} f(x|\mu, \sigma_1^2) dx$, further simplified as (10), as shown at the bottom of next page. According to Eq. (3.322.2) in [17], one has $W_1 = \int_0^\infty e^{-\frac{(2x-\mu)^2}{2\sigma_1^2}} e^{-\frac{(x-\mu)^2}{2\sigma_1^2}} dx = e^{-\frac{\mu^2}{\sigma_1^2}} \sqrt{\frac{\pi\sigma_1^2}{10}} e^{\frac{9\mu^2}{10\sigma_1^2}} \left[1 - \text{erf} \left(\frac{-3\mu}{\sqrt{10}\sigma_1} \right) \right]$. The terms W_2 , W_3 and W_4 can be obtained in a similar manner. Therefore, (10) can be simplified as (11), as shown at the bottom of next page.

According to the analysis in Section II, P_ψ is larger than P_d in high SNR ranges. In (6), it is clear that $1 - P_\psi < 1$ and $\frac{2^{\lfloor \log_2 C(N,p) \rfloor - 1}}{2^{\lfloor \log_2 C(N,p) \rfloor} - 1} \leq 1$. Thus, one has $P_{I,p} < \frac{1}{2} P_\psi + P_\psi < 2P_\psi$. Substituting the above results and (11) into (7), the upper bound of P_I is obtained. The upper bound of P_B can be obtained in a similar way. Finally, the upper bound of P_T is deduced by substituting P_I and P_B into (3). Note that P_T^{multi} is an average version of P_T , where the word ‘‘average’’

TABLE III
COMPARISONS OF DATA RATE AND ENERGY EFFICIENCY

Systems	JPCM-DCSK ($N = 4, P = 2$)	JPCM-DCSK ($N = 4, P = 3$)	RP-MDCSK ($N = 4, M_o = 2$)
Data Rate	5	6	1
EE	$\frac{35}{11}$	$\frac{19}{9}$	$\frac{1}{5}$

refers to statistical averaging over the probability distribution of Rayleigh fading. Specifically, P_T^{multi} is degraded to P_T when $L = 1$ and $\alpha_l = 1$. Therefore, the upper bound of P_T is sufficient to determine the effect of different system parameters on the BER performance of JPCM-DCSK.

C. Data Rate and Energy Efficiency Analysis

In this subsection, the data rate and energy efficiency of JPCM-DCSK are analyzed and then compared to RP-MDCSK. The total number of transmitted bits per symbol is used to evaluate the data rate. Clearly, the data rate of JPCM-DCSK is $\partial = \lfloor \log_2(\sum_{p=1}^P 2^p C(N, p)) \rfloor$, while the data rate of RP-MDCSK is $\partial_R = \log_2 M_o$, where M_o is the modulation order.

Generally, the energy efficiency of DCSK-based systems can be evaluated by the data-energy-to-bit-energy ratio (DBR) [18]. The DBR is defined by $DBR = \frac{E_{data}}{E_b}$, where E_{data} is the energy used to transmit the data-bearing signal and E_b is the bit energy. According to the principle of JPCM shown in Table I and the corresponding analysis in Section II, there are 2^p different cases for the information-bearing signals when p time slots are used to transmit the information bits. Note that the number of time slots used to transmit the information-bearing signals is changed from 1 to P . Therefore, the averaged bit energy of JPCM-DCSK is obtained as $E_b = \frac{\sum_{p=1}^P 2^p C(N, p) [(1+p) \sum_{l=1}^L \alpha_l^2 c(c)^T]}{\partial \sum_{p=1}^P 2^p C(N, p)}$. Moreover, the averaged energy used to transmit the data-bearing signals is computed as $E_{data} = \frac{\sum_{p=1}^P 2^p C(N, p) [p \sum_{l=1}^L \alpha_l^2 c(c)^T]}{\sum_{p=1}^P 2^p C(N, p)}$. Therefore, the DBR of

JPCM-DCSK is $DBR_1 = \frac{E_{data}}{E_b} = \frac{\partial \sum_{p=1}^P p 2^p C(N, p)}{\sum_{p=1}^P (1+p) 2^p C(N, p)}$.

The RP-MDCSK system needs to transmit piecewise-replicated signals to combat impulsive noise, but these signals transmit the same information bits, thus decreasing the energy efficiency. According to [6], the bit energy of RP-MDCSK is $E_b = \frac{(1+N) \sum_{l=1}^L \alpha_l^2 c(c)^T}{\log_2 M_o}$. Note that the piecewise-replicated signals transmit the same information bits, and the energy of data-bearing signal is $E_{data} = \sum_{l=1}^L \alpha_l^2 c(c)^T$. Thus, the DBR of RP-MDCSK is calculated as $DBR_2 = \frac{E_{data}}{E_b} = \frac{\log_2 M_o}{1+N}$.

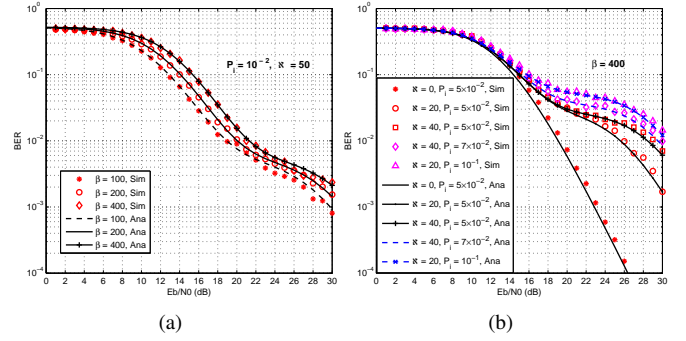


Fig. 2. BER performance of JPCM-DCSK over a multipath PLC channel.

Table III shows the data rate and energy efficiency of JPCM-DCSK and RP-MDCSK when $N = 4$. It is clear that both data rate and energy efficiency of JPCM-DCSK outperform that of RP-MDCSK. As shown in Table III, when $N = 4$ and $P = 3$, JPCM-DCSK only needs 4 information-bearing time slots to transmit 6 information bits so that 2 additional bits are transmitted. Therefore, the data rate of JPCM-DCSK is improved. According to the principle of JPCM shown in Table I, only some information-bearing time slots are used to transmit signal $+c$ or $-c$, while other time slots transmit the zero signal 0 with zero energy. In other words, JPCM-DCSK needs less energy to transmit the same or even more information bits compared to RP-MDCSK. Therefore, the energy efficiency of JPCM-DCSK is improved.

IV. NUMERICAL RESULTS AND DISCUSSIONS

In this section, the BER performance of JPCM-DCSK over the PLC channel is evaluated and compared to that of RP-MDCSK [6], CIM-MC-MDCSK [8] and DPI-DCSK [9]. In simulations, a three-path Rayleigh fading PLC channel with power coefficients $[5/12, 4/12, 3/12]$ is used and its delays are distributed according to uniform distribution ranging from 0 to $4T_c$, where T_c is the chip duration. In Figs. 2 and 3, “Sim” and “Ana” denote the simulation and analytical results, respectively. The analytical results are obtained by (9).

Fig. 2(a) shows the BER performance of JPCM-DCSK over the multipath PLC channel. The system parameters are $N = 4$ and $P = 2$. A good agreement between simulation results and analytical ones verifies the correctness of the theoretical analysis. In Fig. 2(a), a higher β degrades the BER performance of JPCM-DCSK. There is an error floor in Fig. 2(a), because the high-power impulsive noise penalizes the BER performance of JPCM-DCSK.

$$\begin{aligned}
 P_\psi &\approx \int_0^\infty \left\{ 1 - \frac{1}{2} \left[\operatorname{erf} \left(\frac{2x - \mu}{\sqrt{2\sigma_1^2}} \right) + \operatorname{erf} \left(\frac{2x + \mu}{\sqrt{2\sigma_1^2}} \right) \right] \right\} \frac{1}{\sqrt{2\pi\sigma_1^2}} \left\{ \exp \left[-\frac{(x - \mu)^2}{2\sigma_1^2} \right] + \exp \left[-\frac{(x + \mu)^2}{2\sigma_1^2} \right] \right\} dx \\
 &\stackrel{\operatorname{erf}(x) = 1 - \operatorname{erfc}(x)}{\leq} \frac{1}{\sqrt{8\pi\sigma_1^2}} \int_0^\infty \underbrace{\left[\exp \left(-\frac{(2x - \mu)^2}{2\sigma_1^2} \right) + \exp \left(-\frac{(2x + \mu)^2}{2\sigma_1^2} \right) \right]}_{A_1} \underbrace{\left[\exp \left(-\frac{(x - \mu)^2}{2\sigma_1^2} \right) + \exp \left(-\frac{(x + \mu)^2}{2\sigma_1^2} \right) \right]}_{A_2} dx \\
 &\quad \underbrace{\left[\exp \left(-\frac{(x - \mu)^2}{2\sigma_1^2} \right) + \exp \left(-\frac{(x + \mu)^2}{2\sigma_1^2} \right) \right]}_{A_3} \underbrace{\left[\exp \left(-\frac{(x - \mu)^2}{2\sigma_1^2} \right) + \exp \left(-\frac{(x + \mu)^2}{2\sigma_1^2} \right) \right]}_{A_4} dx \\
 &= \frac{1}{\sqrt{8\pi\sigma_1^2}} \underbrace{\int_0^\infty A_1 A_3 dx}_{W_1} + \frac{1}{\sqrt{8\pi\sigma_1^2}} \underbrace{\int_0^\infty A_1 A_4 dx}_{W_2} + \frac{1}{\sqrt{8\pi\sigma_1^2}} \underbrace{\int_0^\infty A_2 A_3 dx}_{W_3} + \frac{1}{\sqrt{8\pi\sigma_1^2}} \underbrace{\int_0^\infty A_2 A_4 dx}_{W_4} \quad (10)
 \end{aligned}$$

$$P_\psi \leq \frac{1}{\sqrt{80}} e^{-\frac{\mu^2}{\sigma_1^2}} \left\{ e^{\frac{9\mu^2}{10\sigma_1^2}} \left[\operatorname{erfc} \left(\frac{3\mu}{\sqrt{10\sigma_1^2}} \right) + \operatorname{erfc} \left(\frac{-3\mu}{\sqrt{10\sigma_1^2}} \right) \right] + e^{\frac{u^2}{10\sigma_1^2}} \left[\operatorname{erfc} \left(\frac{u}{\sqrt{10\sigma_1^2}} \right) + \operatorname{erfc} \left(\frac{-u}{\sqrt{10\sigma_1^2}} \right) \right] \right\} \quad (11)$$

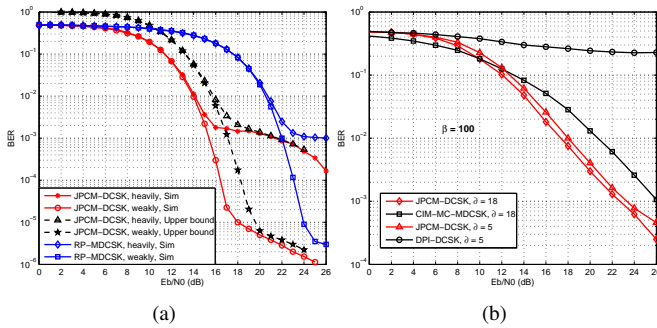


Fig. 3. BER performances of JPCM-DCSK, RP-MDCSK [6], CIM-MC-MDCSK [8] and DPI-DCSK [9].

Fig. 2(b) shows the effects of N and P_i on the BER performance of JPCM-DCSK with $N = 8$ and $P = 2$ over the multipath PLC channel. The analytical results well match the simulation results, further verifying the analysis in the previous section. One can see the slight mismatch results from the approximations in (6) and (8). As shown in Fig. 2(b), when N is increased, i.e., worse impulsive noise is involved in PLC channel, a BER decline takes place in BER performance. Furthermore, a higher occurrence probability of impulsive noise also incurs BER performance degradation.

In Fig. 3(a), the BER performance of JPCM-DCSK is compared to that of RP-MDCSK over a PLC channel. Note that RP-MDCSK outperforms direct sequence differential phase shift keying (DS-DPSK) in BER performance [6], and RP-MDCSK is chosen for comparison. Fig. 3(a) displays the BER for heavily impulsive noise ($IAT = 0.0196$ s, $T_p = 0.0641$ ms) and weakly impulsive noise ($IAT = 8.1967$ s, $T_p = 0.1107$ ms) scenarios [3], where IAT denotes the inter arrival time which is a reciprocal of λ . The simulation parameters are $N = 4$, $P = 3$, $\beta = 100$ and $N = 20$. Moreover, $M_o = 2$ is used in the simulations of RP-MDCSK. The upper bound BERs in Fig. 3(a) are obtained in Subsection III-B. It is clear that the upper bound BERs match the simulated BERs in high SNR regions, verifying the correctness of the derivations. Moreover, JPCM-DCSK has better BER performance than RP-MDCSK for both heavily and weakly impulsive noise scenarios.

As shown in Fig. 3(b), the BER performance of JPCM-DCSK is compared to that of CIM-MC-MDCSK and DPI-DCSK over the multipath PLC channel with heavily impulsive noise. All systems have the same number of transmitted bits per symbol. CIM-MC-MDCSK is a multicarrier modulation scheme, where the number of subcarriers is set to 4 in simulation. When $\partial = 18$, multicarrier modulation is also used in JPCM-DCSK and the system parameters are $N = 4$ and $P = 3$. Furthermore, when $\partial = 5$, the simulation parameters of JPCM-DCSK are $N = 4$ and $P = 2$. Clearly, DPI-DCSK has a high error floor because impulsive noise makes different permuted chaotic sequences basically not orthogonal to each other. JPCM-DCSK offers about 3 dB performance gain compared to CIM-MC-MDCSK at $BER = 10^{-3}$.

V. CONCLUSION

A joint position and constellation mapping assisted DCSK system has been proposed to address the problem of unreliable data transmission in the PLC channel subjected to Laplacian impulsive noise. The positions of information-bearing time slots and the constellation of BPSK modulated symbol are

jointly mapped to a stream of transmitted bits, which enables JPCM-DCSK to obtain higher data rate and energy efficiency. In addition, an effective joint position and constellation detection algorithm has been developed. With this algorithm, the JPCM-DCSK receiver can distinguish the positions of information-bearing and unused time slots, such that the information bits can be retrieved by different constellation states and time slot positions. The BER expression of JPCM-DCSK has also been derived over the PLC channel, and its correctness has been confirmed by the simulation results. It is concluded that the proposed JPCM-DCSK system performs better in both BER performance and energy efficiency than RP-MDCSK. Therefore, JPCM-DCSK can be a good candidate for narrowband PLC transmission links.

REFERENCES

- [1] M. Nassar, J. Lin, Y. Mortazavi, A. Dabak, I. H. Kim, and B. Evans, "Local utility power line communications in the 3-500 KHz band: Channel impairments, noise, and standards," *IEEE Signal Process. Mag.*, vol. 29, no. 5, pp. 116-127, Sept. 2012.
- [2] Y. H. Ma, P. L. So, and E. Gunawan, "Performance analysis of OFDM systems for broadband power line communications under impulsive noise and multipath effects," *IEEE Trans. Power Del.*, vol. 20, no. 2, pp. 674-682, Apr. 2005.
- [3] A. Mathur, M. R. Bhatnagar, and B. K. Panigrahi, "Performance evaluation of PLC under the combined effect of background and impulsive noises," *IEEE Commun. Lett.*, vol. 19, no. 7, pp. 1117-1120, Jul. 2015.
- [4] G. Kolumbán, G. K. Vizvari, W. Schwarz, and A. Abel, "Differential chaos shift keying: A robust coding for chaos communication," in *Proc. Nonlinear Dyn. Electron. Syst.*, Seville, Spain, 1996, pp. 92-97.
- [5] G. Kaddoum and N. Tadayon, "Differential chaos shift keying: A robust modulation scheme for power-line communications," *IEEE Trans. Circuits Syst. II, Exp. Briefs*, vol. 64, no. 1, pp. 31-35, Jan. 2017.
- [6] M. Miao, L. Wang, G. Chen and W. Xu, "Design and analysis of replica piecewise M-ary DCSK scheme for power line communications with asynchronous impulsive noise," *IEEE Trans. Circuits Syst. I, Reg. Papers*, vol. 67, no. 12, pp. 5443-5453, Dec. 2020.
- [7] X. Cai, W. Xu, M. Miao and L. Wang, "Design and performance analysis of a new M-ary differential chaos shift keying with index modulation," *IEEE Trans. Wireless Commun.*, vol. 19, no. 2, pp. 846-858, Feb. 2020.
- [8] G. Cai, Y. Fang, J. Wen, S. Mumtaz, Y. Song and V. Frasca, "Multi-carrier M-ary DCSK system with code index modulation: An efficient solution for chaotic communications," *IEEE J. Sel. Topics Signal Process.*, vol. 13, no. 6, pp. 1375-1386, Oct. 2019.
- [9] S. Liu, P. Chen and G. Chen, "Differential permutation index DCSK modulation for chaotic communication system," *IEEE Commun. Lett.*, vol. 25, no. 6, pp. 2029-2033, Jun. 2021.
- [10] T. Bai et al., "Fifty years of noise modeling and mitigation in power-line communications," *IEEE Commun. Surveys Tuts.*, vol. 23, no. 1, pp. 41-69, 1st Quart. 2021.
- [11] M. Zimmermann and K. Dostert, "Analysis and modeling of impulsive noise in broad-band powerline communications," *IEEE Trans. Electromagn. Compat.*, vol. 44, no. 1, pp. 249-258, Feb. 2002.
- [12] T. Shongwe, A. H. Vinck, and H. C. Ferreira, "A study on impulse noise and its models," *SAIEE Africa Res. J.*, vol. 106, no. 3, pp. 119-131, 2015.
- [13] S. Prakash, A. Bansal, and S. K. Jha, "Performance analysis of narrowband PLC system under Gaussian Laplacian noise model," in *Proc. Int. Conf. Elect., Electron., Optim. Techn.*, Mar. 2016, pp. 3597-3600.
- [14] N. Agrawal, P. K. Sharma, and T. A. Tsiftsis, "Multihop DF relaying in NB-PLC system over rayleigh fading and Bernoulli-Laplacian noise," *IEEE Syst. J.*, vol. 13, no. 1, pp. 357-364, Mar. 2019.
- [15] M. Antoniali, F. Versolatto, and A. M. Tonello, "An experimental characterization of the PLC noise at the source," *IEEE Trans. Power Del.*, vol. 31, no. 3, pp. 1068-1075, Jun. 2016.
- [16] R. J. Marks, G. L. Wise, D. G. Haldeman, and J. L. Whited, "Detection in Laplace noise," *IEEE Trans. Aerosp. Electron. Syst.*, vol. AES-14, no. 6, pp. 866-872, Nov. 1978.
- [17] I. S. Gradshteyn and I. M. Ryzhik, *Table of Integrals, Series and Products*, 7th ed. San Diego, CA, USA: Academic, 2007.
- [18] G. Kaddoum, F. Richardson, F. Gagnon, "Design and analysis of a multicarrier differential chaos shift keying communication system," *IEEE Trans. Commun.*, vol. 61, no. 8, pp. 3281-3291, Aug. 2013.